X3 Expansion Tube Driver Gas Spectroscopy and Temperature Measurements

Viha Parekh[1], David Gildfind[2], Steven Lewis[3] and Christopher James[4]
The University of Queensland, St Lucia, Queensland, 4072

The University of Queensland's X3 facility is a large, free-piston driven expansion tube used for superorbital and high Mach number scramjet aerothermodynamic studies. X3's powerful test flow is initiated by firing its heavy piston into its driver gas – a mixture of argon and helium. Knowledge of the initial and transient temperature behavior of the driver gas is critical to correctly characterize the driver performance, losses and all subsequent expansion tube flow processes. However, the driver gas temperature is not currently measured during routine experimentation and there is limited evidence of its measurement in other international facilities. During recent scramjet flow development in X3, lower than expected experimentally measured shock speeds through helium indicated an effective driver temperature of approximately 2400 K, compared to a temperature of 3743 K at the time of diaphragm rupture for an ideal isentropic driver gas compression. These performance losses motivate this study, which examines initial and peak driver gas temperatures. The study shows that the initial steady-state driver gas temperature, once the filling process ceases, can be approximated by the external driver tube wall temperature. During filling, a net increase in driver gas temperature occurs due to compression heating, as well as, Joule-Thomson effect for helium. Optical emission spectroscopy was then used to resolve the peak driver gas temperature, during piston compression, for a Mach 10 scramjet operating condition. The driver gas emission spectrum exhibits a significant background radiation component, with prominent spectral lines attributed to contamination of the flow. A blackbody approximation of background radiation suggests a peak driver gas temperature of 3200±100 K. Application of the line-ratio method to two argon lines at 763.5 and 772.4 nm suggests a temperature of 3500±750 K. Comparison of these estimates to the ideal isentropic driver gas temperature at diaphragm rupture, 3743 K, suggests losses in the driver gas temperature during the compression process are not extensive for X3, and further that the lower than expected shock speeds are likely primarily due to pressure losses during driver gas expansion through the diaphragm and at the driver-to-driven tube area change.

Nomenclature

A = Einstein coefficient for spontaneous emission, s^{-1}
a = sound speed, m/s
c = speed of light = 3×10^8 m/s
E = energy of the upper atomic state, eV
g = statistical weight of upper atomic state
h = Planck's constant = 4.136×10^{-15} eV.s
I = spectral intensity, counts
K = Boltzmann's constant = 8.617×10^{-5} eV/K
L = spectral radiance, W/m^2/sr/nm
M = molecular weight, g/mol
P_i = driver gas initial pressure, Pa
P_p = driver gas pressure at rupture, Pa
R = gas constant, J/mol/K
T_{abs} = absolute temperature, K
T_{ex} = excitation temperature, K
T_i = driver gas initial temperature, K
T_p = driver gas average peak temperature, K
γ = ratio of specific heats
λ = wavelength, m

[1] Undergraduate, School of Mechanical and Mining Engineering, AIAA Student Member
[2] Lecturer, Centre for Hypersonics, School of Mechanical and Mining Engineering
[3] PhD Candidate, Centre for Hypersonics, School of Mechanical and Mining Engineering
[4] PhD Candidate, Centre for Hypersonics, School of Mechanical and Mining Engineering

I. Introduction

IMPULSE facilities provide the unique capability to reproduce the high total pressure and high velocity flows which are associated with scramjet-powered access to space and planetary re-entry trajectories. These flows can be used for aerothermodynamic studies to: improve physical models of the flow around hypersonic vehicles, develop and validate computational fluid dynamics (CFD) codes and verify design concepts prior to flight testing. Currently, the University of Queensland's (UQs) X3 impulse facility is the world's highest performance expansion tube [1, 2].

A free-piston driven facility, X3's test flow is driven by a shock wave which initiates from firing a heavy piston into its driver gas and blasting the gas through a diaphragm. Characterizing properties of the flow throughout the facility, however, is difficult; the high-temperature and high-velocity test flow provides a harsh environment in which to establish instrumentation, limiting the types of direct measurements that can be made. Routine characterization of flow properties relies on static pressure measurements, by flush mounted piezoelectric pressure core barrel (PCB) transducers recessed in the tube walls along X3's length. Average shock speeds can then be calculated from time-of-arrival of the shock at each transducer, and along with the time-resolved pressure measurements, provide the basis for analytical studies and/or CFD reconstructions of flow through the entire facility.

A persistent source of uncertainty in CFD simulations are the poorly defined boundary conditions of the free-piston driver, i.e. the piston and driver gas. Flow properties here directly determine the flow conditions downstream [3]. In particular, the driver gas temperature is a critical determinant of final shock speed – which is, in turn, an indicator of overall facility performance. This paper reports the peak driver gas temperature for X3's "x3-scr-m10p0a-rev-0" condition [4], a Mach 10 scramjet flow condition, by measuring the emission spectrum of the driver gas. Since the eventual temperature of the driver gas is directly proportionate to its initial value, the initial fill temperature of the driver gas is also studied, over the duration of its filling into the compression tube and just prior to the piston stroke.

Gildfind et al. [5] derived an analytical technique to calculate an 'effective' driver temperature at the time of primary diaphragm rupture, appropriate for tuned drivers (see *section II* for a description of tuned driver operation), using experimentally measured shock speeds through a helium test gas. The technique assumes that along with pressure, temperature remains constant for a short duration after rupture, under tuned operation of the driver. Using the experimentally measured driver pressure after diagram rupture for the Mach 10 flow condition, this methodology suggests an effective driver temperature of approximately 2400 K, which is significantly lower than that for an ideal, isentropic compression, 3743 K (see *section IV-C* for calculation). This observed difference motivates the work described in this paper.

II. X3 Expansion Tube

In its simplest form, a free-piston driven expansion tube comprises three sections: (i) the *driver* containing the driver gas (a mixture of the monatomic gases, helium and argon); (ii) the *shock tube* containing the test gas; and, (iii) the low-pressure *acceleration tube* containing the test piece at its exit [6]. These tube sections are separated by two diaphragms; the first of these diaphragms (between sections i and ii) is capable of withstanding high pressures and is typically constructed from steel or aluminum, whilst the latter (between sections ii and iii) has a pressure threshold just sufficient to contain the test gas.

Compression of the driver gas to a high pressure and temperature causes rupture of the first diaphragm, initiating shock-tube flow. As a result, the high-pressure, hot driver gas propagates a shock wave into the test gas, rapidly compressing it and accelerating it down the tube. The test gas then breaches the secondary diaphragm, driving a shock into the relatively low-pressure acceleration tube, driven by a region of expanding test gas. Simultaneously, an unsteady expansion wave processes the test gas and the gas propagates downstream toward the test section. The useful flow interval begins when the downstream edge of the expanded test gas reaches the test piece; and ends at the arrival of the downstream edge of the unsteady expansion. The current X3 configuration incorporates a secondary driver which consists of an additional volume of gas (helium) between the primary diaphragm and test gas, to improve performance [7], however is not discussed here. A schematic of X3's current configuration and the evolution of flow processes is shown in Fig. 1.

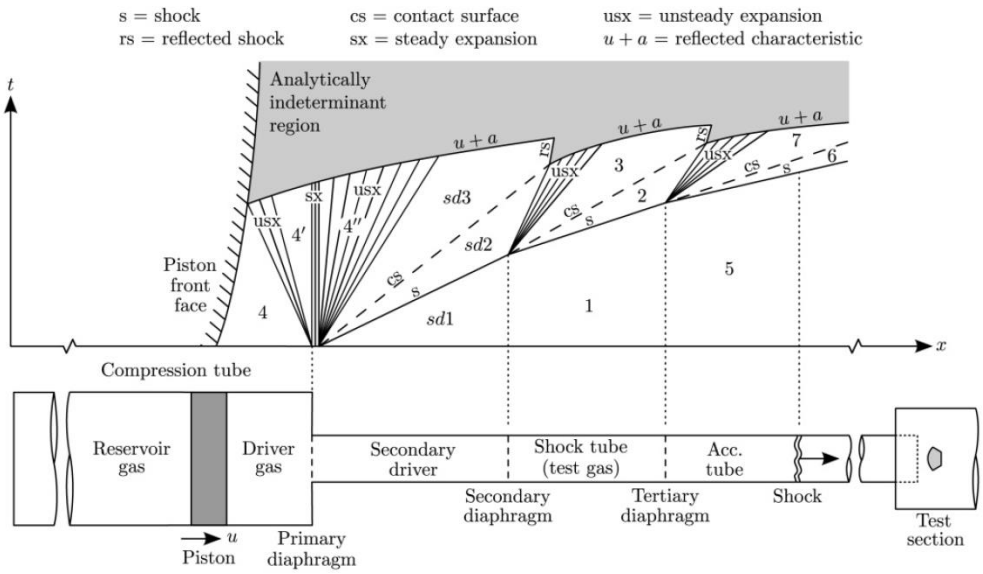

Figure 1. Flow processes in a free-piston driven expansion tube with a secondary driver (not to scale) [1].

For free-piston driven facilities such as X3, the driver gas flow is powered by firing a piston into the driver gas. The piston is accelerated by a reservoir of compressed air, gaining substantial velocity as it traverses the compression tube; for example, X3's piston reaches velocities exceeding 140 m/s [1]. The stroke significantly increases both the driver gas pressure and compression ratio, until the pressure threshold of the primary diaphragm is reached and rupture occurs. A desired, approximately constant driver gas pressure level and temperature can be maintained over the useful test time by operating the piston under a *tuned condition* [8, 9]. Here, the piston is slightly over-driven such that its speed at rupture is moderately greater than that required to compensate for driver gas flow through the ruptured diaphragm to the driven tube. The driver gas pressure is designed to rise to about 10% more than the rupture pressure and as a result tends to reduce minimally during the useful supply time [5]. There are, however, fluctuations in the driver gas pressure which occur at much shorter timescales (e.g. ~100 μs [4]) due to reflection of compression waves generated during the piston stroke, as well as, the expansion fan propagated into the driver gas at the primary rupture event [10].

The strength of the shock propagated into the driven gas, predominantly depends on the ratio of the sound speed in the driver and driven gases:

$$a = \sqrt{\gamma R T_i} = \sqrt{\gamma \frac{R_{universal}}{M} T_i}$$

For a particular driven gas, shock strength can be maximized by minimizing driver gas molecular weight and increasing initial driver gas temperature. Helium provides a high sound speed due to its relatively low molecular weight (4 g/mol compared to 40 g/mol for argon); however argon (which has the same specific heat ratio as helium) is often used as a diluent, as the piston velocities required to match driver gas venting at these high sounds speeds in helium, are often difficult to attain.

III. Initial driver gas temperature

Current experimental approaches to measuring the initial temperature of the driver gas assume it is at the, often unmeasured, 'ambient condition'. Mee [11] estimated that ambient facility temperature varies from about 291 K to 303 K (as reported for UQ's T4 facility in Brisbane, Australia), proposing an accuracy of ± 2% in fill temperature when unmeasured. Miller & Jones [12] measured the driver gas temperature for a fixed volume helium driver using the National Aeronautics and Space Administration's (NASAs) Langley 6-inch expansion tube; the experiments validated that higher initial driver gas temperatures provide increased shock velocity, due to the increased rupture temperature for the same compression ratio. In this case, higher driver gas temperatures were attained by allowing a relatively small time lapse between fill and diaphragm rupture. The study observed that during filling from the storage bottle to the compression tube, the driver gas temperature rose, suggesting this was due to Joule-Thomson heating as well as compression heating; once the fill valve was shut, the temperature decayed to ambient condition.

A. Methods

The driver gases – argon and helium – are stored at ambient temperature in gas bottles, at up to 20 MPa. During filling of the compression tube, the gas undergoes free expansion from these high pressures (megapascals) to less than atmospheric pressure (kilopascals) in the initially evacuated compression tube, via a manually regulated throttling valve. In this study, measurement of the initial driver gas fill temperature encompassed two experiments: the first of these established a thermocouple set-up in the wall of the compression tube to measure the internal tube temperature, as well as, the ambient facility temperature, during the driver gas filling process. To simulate driver gas filling, the primary diaphragm was installed to isolate the compression tube and the reservoir was vented to prevent piston launch. Pure argon and pure helium gas fills to 30 kPa into an initially evacuated compression tube were each examined separately, to ascertain the limits for temperature variations in typical driver gas mixtures of the two gases. Following both fills, the compression tube was vented to atmospheric conditions, establishing the baseline temperature within the compression tube. An apparent correlation between the internal tube temperatures with the tube wall temperature motivated a second experiment. Here, the external tube wall was monitored over a period of eight days using surface thermocouples, as well as, the internal tube and ambient temperatures.

B. Results

Internal tube and ambient temperatures during simulation of the driver gas fill are shown in Fig. 2, along with digital gauge readings of the compression tube pressure at key time intervals.

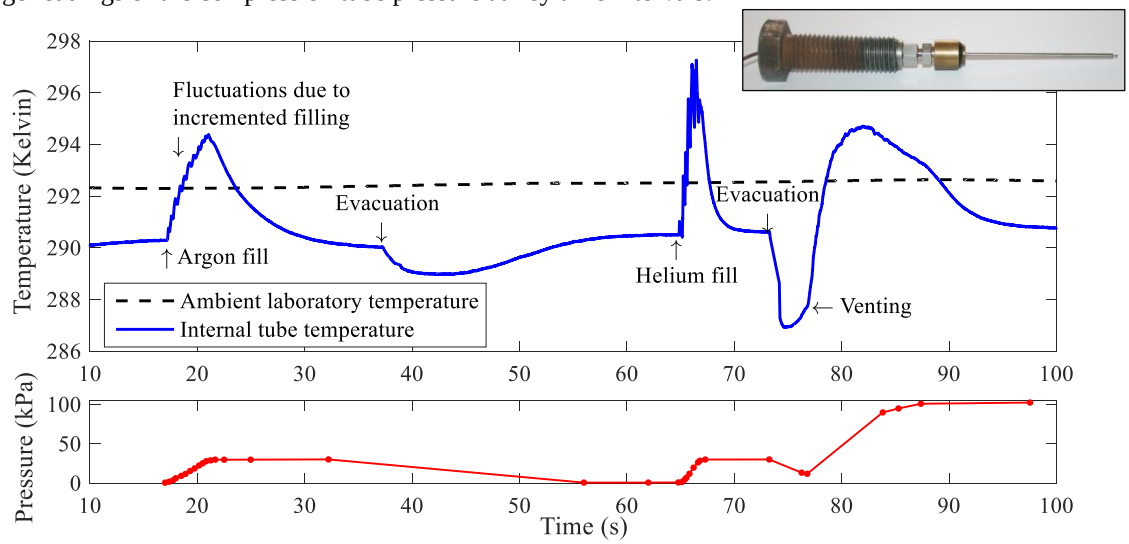

Figure 2.Temperature and pressure variation during simulation of the driver gas filling process. *Internal compression tube temperature is monitored via an exposed junction, type-T thermocouple (shown) 0.2 m upstream of the primary diaphragm. Data is acquired at 10 ms intervals using Pico Technology's TC-08 thermocouple data logger and PicoLog software, with an internal cold junction providing a reading of the ambient room temperature.*

In Fig.2, a net rise in the internal compression tube temperature during driver gas fill is apparent and is consistent with Miller & Jones' [12] observations. This temperature rise is approximately 4 K for argon, compared to 7 K for helium. Two mechanisms of driver gas heating are suggested:

1. Compression heating: At the near-ambient temperatures observed, Joule-Thomson expansion of argon predicts a temperature decrease during expansion. Thus the measured increase in its temperature instead suggests compression heating of the driver gas during fill; the volume of gas in the driver section is continuously being compressed by the inflow and the resulting work on the fluid volume causes a net increase in temperature. During venting (i.e. a rapid inflow of air) a temperature rise of similar magnitude (to argon) is observed until atmospheric pressure is attained, after which temperature decays; again, indicating compression heating.
2. Joule-Thomson effect: Joule-Thomson expansion predicts a temperature increase during throttling of helium at ambient temperatures; and hence, is a likely (partial) contributor to the temperature rise observed during the helium fill, in addition to compression heating described above.

Once the desired fill pressure was achieved and the tube was isolated, the driver gas temperature rapidly decreases to an approximately constant value, below the ambient temperature. Note that this same value is attained for all evacuation and fill conditions, suggesting that its measurement is a useful indicator for the initial driver gas temperature. The timescales over which temperature decay occurs are much shorter for helium (~5 minutes) than argon (~15 minutes), due to the higher thermal conductivity of the former; i.e. an intermediate time interval will be required for mixtures of the two gases. In practice, the lapse between driver gas filling and piston launch is 5 to 10 minutes. From Fig. 2 argon decayed to within 1.2 K of its steady-state temperature after approximately 5 minutes after filling. This corresponds to a difference of less than 0.5% between the true and steady-state temperature; which is a significantly better estimate of the initial driver gas temperature than assuming an unmeasured ambient temperature. Study of the internal and surface compression tube temperatures along with the ambient temperature, with the tube vented to atmospheric pressure, showed that internal tube temperature tracks closely with the tube wall temperature (Fig. 3).

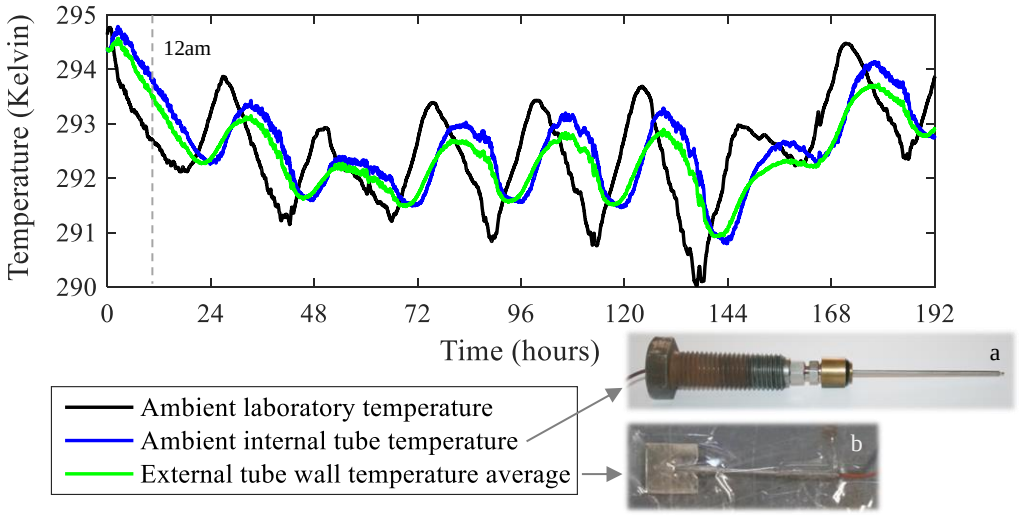

Figure 3.Internal, tube wall and ambient temperatures over eight days, as well as, internal tube (a) and surface (b) thermocouple fittings. *Two type-T surface thermocouples were used to monitor the tube external tube wall temperature and the average reading is shown here. Data is acquired once per minute, with internal driver tube and ambient laboratory temperatures measured as previously set-up.*

Ambient temperature minima and maxima precede both the internal and tube wall temperature peaks typically by 5.5 to 6.5 hours, since the volume of the tube wall provides a significant thermal mass. As a result, the tube temperature may be above or below the ambient condition; however, during the typical timeframes during which the facility is operated (i.e. during the day), the tube temperature is less than ambient temperature, as observed for the driver gas fill tests in Fig. 2. Finally, the ambient temperature in the expansion tube laboratory varies between approximately 290 K and 295 K over the experiment duration, suggesting the lower limit for annual temperature variation in the X3 facility slightly exceeds Mee's [11] estimation for the T4 facility. If International Standard Atmosphere (ISA) temperature (293.15 K) is assumed here, these measurements suggest an uncertainty in the initial driver gas temperature of ±1 %. Thus, these results do not indicate that the initial driver gas temperature is responsible for the observed low shock speeds.

IV. Driver gas spectroscopy

Emission spectroscopy has been used in several experiments at UQ to observe the spectra of radiating flows around test models, particularly in the X2 facility [13-17]; both ratio-pyrometry and blackbody approximations have been used for temperature estimation [13, 14]. Contamination of test gas flow is persistent: Eichmann [13] shows calcium contamination from a Mylar secondary diaphragm; a range of spectral lines due to neutral and singly ionized iron from damage to the test model rather than particles stripped from the tube walls; and a sodium doublet due to contamination from vacuum grease. An emission study of air test flow in the now-decommissioned X1 (UQ), observed significant radiation from entrainment of metallic contaminants (such as calcium and iron) in the flow at a

moderate enthalpy condition (14 MJ/kg) [18]. At a higher enthalpy condition (93 MJ/kg), whilst some atomic lines persisted, a broadband background component was apparent; ion-electron recombination and bremsstrahlung (radiation emitted when a high speed electron loses its energy in collisions with another charged particle) were suggested as the likely contributors, indicating the presence of electrons, as well as, weaker atomic lines whose peaks were obscured by the background.

Although there are a limited number of studies which report on the use of line-ratio techniques in impulse facilities, line-ratio techniques have been used to study combustion, plumes and plasmas; for example by Devia et al. [19]. A number of examples of shock tube spectroscopic measurements use more complex techniques, such as interferometry, planar laser-induced fluorescence (PLIF) [20] and tuneable diode laser absorption spectroscopy (TDLAS) [21]; however, due to the limited available data on driver gas spectra, this study focuses on optical emission spectroscopy. Stagnation temperatures have been measured in the test section of reflected shock tunnels using total temperature probes in various configurations [22-24], although at much lower temperatures than in this study.

For an optically thick medium (ie. light is readily absorbed) the emission spectrum is continuous and uniquely dependent on temperature. Such media can be approximated by a blackbody – the perfect emitter and absorber; radiance of spectral emission is described by Planck's blackbody distribution [25]:

$$\mathrm{L} = \frac{2\mathrm{hc}^2}{\lambda^5}\frac{1}{\mathrm{e}^{\mathrm{hc}/\lambda \mathrm{k} \mathrm{T}_{\mathrm{abs}}} - 1}$$

The line spectra generated from transition of atoms between discrete energy levels in a radiating gas tends to be an opposite extreme to the continuous blackbody radiation curves, as the optical density of the radiating gas decreases [25]. For an optically thin species (i.e. light readily passes through), discrete energy level transitions of atoms, i.e. quantum mechanical interactions between electrons orbiting atoms and photons of light, produce spectral lines at distinct wavelengths. These spectra are unique to an atomic species. The Boltzmann distribution may be used to describe the spectral intensity for an atom's transition between a lower energy level (state 1) and upper level (state 2) [19]:

$$\mathrm{I}_{21} = \frac{\mathrm{Nhc}}{\mathrm{U}}.\frac{\mathrm{g}_2\mathrm{A}_{21}}{\lambda_{12}}\mathrm{e}^{-\mathrm{E}_2/\mathrm{kT}_{\mathrm{ex}}}$$

The weighted transition probability (gA) is calculated from product of the statistical weight of the energy of state 2 (g) and the Einstein coefficient for spontaneous emission (A). N (the density of particles of the species), h, c and U (a partition function for the species, which acts as a normalization factor) are the same for atomic lines of the species; hence, the temperature can be calculated from the comparison of the emission intensities for two discrete transitions between energy states, m-n and p-n ($p > m$) for the same species (i.e. $\frac{\mathrm{Nhc}}{\mathrm{U}} = \text{constant}$) [19]:

$$\mathrm{T}_{\mathrm{ex}} = \frac{\mathrm{E}_{\mathrm{m}} - \mathrm{E}_{\mathrm{p}}}{-\mathrm{k}\ln\left(\frac{\mathrm{I}_{\mathrm{mn}}\mathrm{g}_{\mathrm{m}}\mathrm{A}_{\mathrm{mn}}\lambda_{\mathrm{p}}}{\mathrm{I}_{\mathrm{pn}}\mathrm{g}_{\mathrm{p}}\mathrm{A}_{\mathrm{pn}}\lambda_{\mathrm{m}}}\right)}$$

Validity of the method requires: (i) local thermal equilibrium (LTE) to exist, i.e. where de-excitation due to collision is more likely than due to spontaneous emission, (ii) a sufficiently wide range for E and hence λ [19, 25] and (iii) background emission to be adequately excluded from the intensities of the two transitions [26, 27].

A. Methods

Driver gas spectra are acquired using an Acton Research SpectraPro 2300i spectrometer (Princeton Instruments), (Fig. 4a), coupled with a 1024×256 pixel PI-MAX ICCD Camera with a Generation III Unigen II filmless image intensifier. Light is transmitted from the driver section to the spectrometer entrance slit via a 7-fiber fiber-optic bundle. At its source end, a vacuum-tight fitting (Fig. 4b) aligns the bundle inside the tube wall, secured by a heavy bolt. An optical window (made from SCHOTT Borofloat 33 Borosilicate glass) is included in this fitment to prevent damage to the fiber-optic from passing flow; and O-rings installed at the lower and upper surfaces of the window ensure a vacuum-tight seal. At the spectrometer entrance slit, a fiber adapter plate and a lens tube mount the fiber at a distance of about 5 mm from the slit.

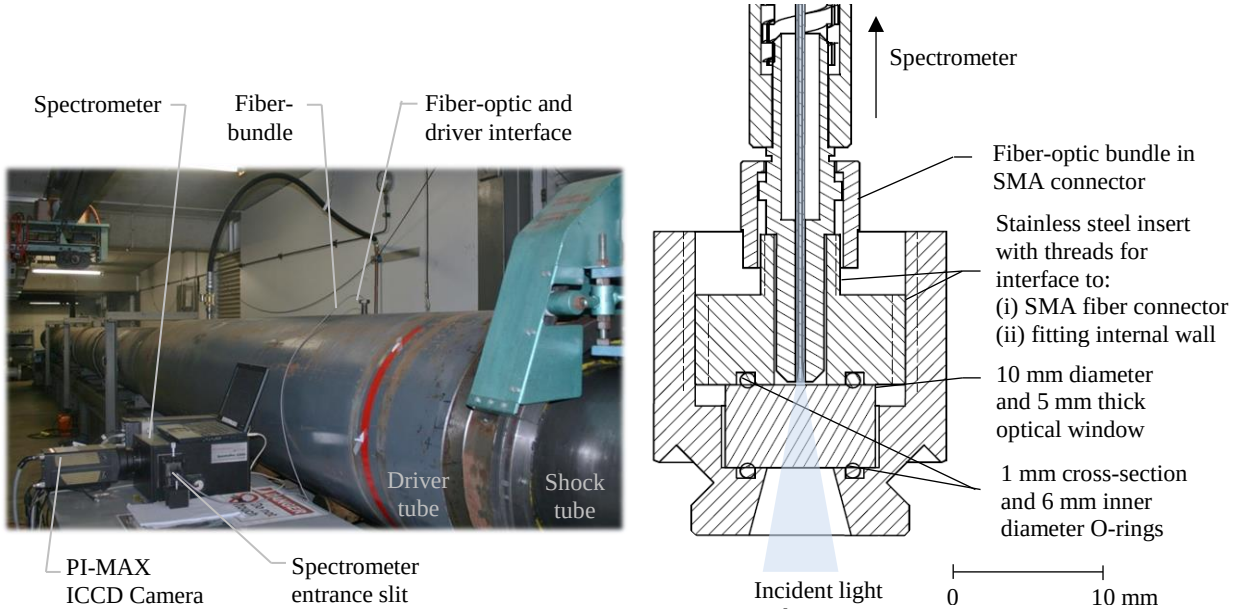

Figure 4.(A) X3 driver section and spectrometer set-up and (B) Fiber-optic and driver tube interface.

The spectral output of the spectrometer was calibrated by comparing the true and measured spectral irradiances of a broad spectrum tungsten-halogen 1000 W OL200M lamp (Optronic Laboratories), imaged with the external optics in place. The calibration ensures the relative intensities of the spectra at various wavelengths are correctly reported; however since the capture angle at the source is not accurately known, the calibrated spectral intensities are reported as normalized. The alignment of the spectrometer wavelengths was validated using a mercury lamp, with known lines at 435.8, 546.1 and 794.5 nm [28].

Spectra are acquired near the peak driver gas temperature – which corresponds with peak driver pressures. After the rupture of the primary diaphragm at 17.5 MPa, pressure remains close to its peak value for ~150 μs. Assuming isentropic processes, temperature is then also expected to remain relatively constant over this period, despite the observed pressure fluctuations. Therefore, the spectrometer is triggered to coincide with this period of constant pressure, with the rapid rise in secondary driver pressure (ST1) caused by the arrival of the shock. Fig. 5 shows the static pressure behavior in the driver (CT) and secondary driver tubes, for three previous experiments with the same driver condition as in this study. Repeatability across the traces suggests reliability in the triggering set-up; hence the same near-peak pressures can be consistently observed for the condition. This is important for this study, since X3's current set-up does not permit pressure and temperature to be concurrently monitored; in this study, CT is replaced by the fiber-optic fitting (Fig. 4b) required for the spectroscopic measurements.

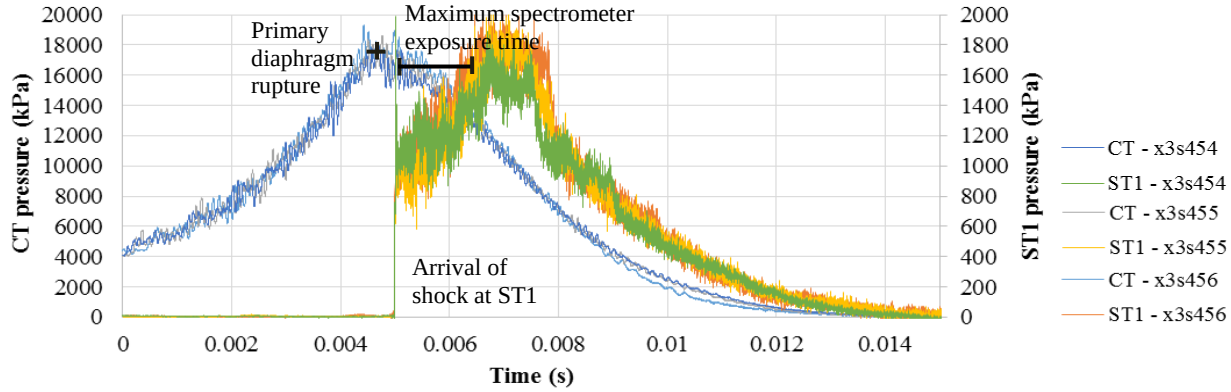

Figure 5. Driver and secondary driver static pressure traces. *CT and ST1 are 0.2 m upstream and 1.68 m downstream of the primary diaphragm, respectively.*

B. Driver gas spectra

A broadband image of the driver gas spectrum is shown in Fig. 6a (for shot x3s470). The doublet near 770 nm was imaged in further detail for shot x3s468 (Fig. 6b).

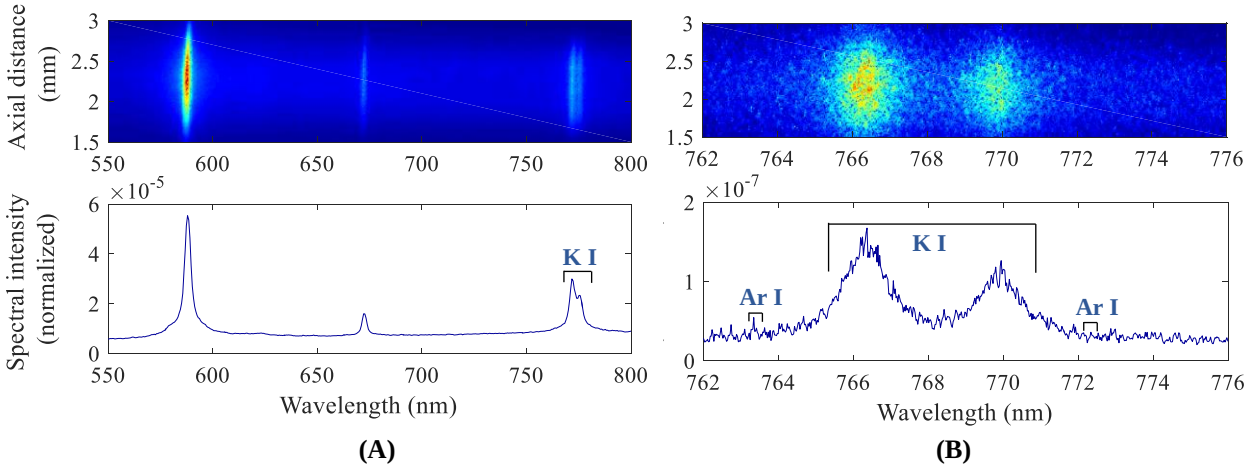

Figure 6. (A) Driver gas spectra for shot x3s470. *Image was acquired with 150 g/mm grating, centered at 700 nm. Exposure =50 µs, gain = 200 and slit width = 50 µm.* **(B) Driver gas spectra for shot x3s468.** *Image was acquired with 1800 g/mm grating, centered at 770 nm. Exposure =150 µs, gain = 250 and slit width = 50 µm. The spectral intensity at each resolved wavelength is calculated by averaging the intensities of the central band of 17 pixels from the spectrum image.*

A distinct feature of the observed spectrum is the large continuum of background radiation (evident especially in Fig. 6a). This may be due to the presence of electrons from atomic collisions or several species radiating at relatively low intensities. The doublet at 766.5 nm and 769.9 nm corresponds well with the spectral features of potassium at these wavelengths. At the finer resolution image (Fig. 6b), an underlying structure of these two spectral lines is suggested; this may be a result of the hyperfine structure of the potassium transitions [29] or a result of other radiating species. The prominent spectral lines observed near 587 nm and 672 nm are unidentified; an initial identification suggested neutral calcium contamination, however a two-line ratio temperature estimate indicated that this was not likely. Therefore, further work is required for their identification, since they may be useful in estimating the driver gas temperature. A substantial amount of broadening is apparent in the observed spectral lines; at the high pressures of the driver gas, pressure broadening is likely the most significant contributor. Evidence for pressure broadening is the presence of the background continuum, which can also result from interactions between particles [18].

Prominent spectral features of argon were not observed, despite argon being a dominant species in the driver gas flow (by concentration). Small peaks in the spectrum near 763.5 nm and 772.4 nm do however correspond with the electronic transitions of argon at these wavelengths. This suggests that whilst argon is a radiator at these temperatures, the majority of its spectral lines are obscured by the continuum.

C. Temperature estimates

As a baseline, the theoretical driver gas temperature at the time of diaphragm rupture can be estimated using isentropic compression theory [30]. The initial temperature is assumed to be at the average tube temperature (293 K), as suggested from the above study of initial driver gas temperature. The initial driver pressure is 30 kPa for the operating condition and the eventual pressure of the gas is given by the rupture pressure of the primary diaphragm (17.5 MPa). The specific heat ratio for a monatomic gas is ~1.67; therefore:

$$\left(\frac{T_p}{T_i}\right) = \left(\frac{P_p}{P_i}\right)^{\frac{\gamma-1}{\gamma}} \rightarrow T_p = (293 \pm 2\ \mathrm{K}) \times \left(\frac{17.5 \times 10^6}{30 \times 10^3}\right)^{\frac{1.67-1}{1.67}} \cong 3743 \pm 25\ \mathrm{K}$$

Comparison of the *shape* of the background radiation to blackbody curves (Fig. 7), assuming an optically thick radiation component, suggests a driver gas temperature is 3200±100 K. This value is 85 % of the isentropic estimate

(3743 K), although much higher than the predicted 'effective' temperature, 2400 K, which is 64 % of the isentropic estimate.

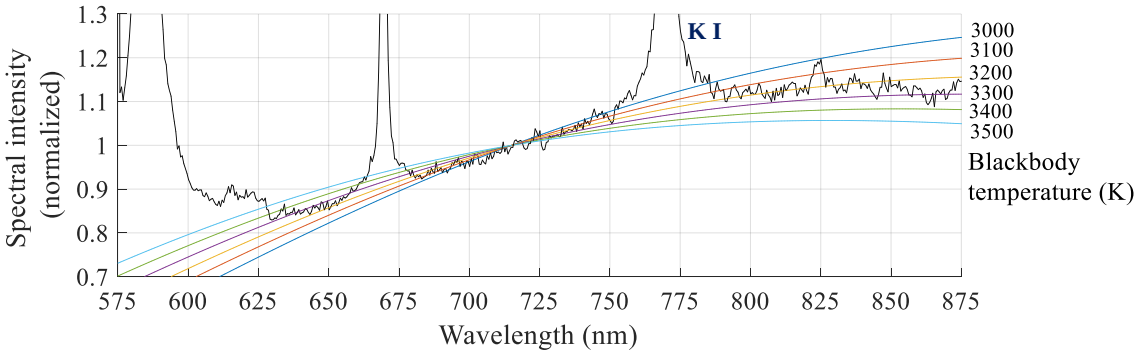

Figure 7. Blackbody curves overlaid on driver gas spectra for shot x3s464. *Spectrum was acquired with 150 g/mm grating, centered at 770 nm. Exposure =150 µs, gain = 200 and slit width = 50 µm. Intensities for both the blackbody and the emission continuum are normalized arbitrarily at 715 nm. Comparisons between the two are based on the spectrum shape and can be made only for continuum wavelengths where broadening due to the peaks is small.*

The two-line ratio method was applied to argon lines at 763.5 and 772.4 nm, suggesting a peak driver gas temperature of 3500 K. The transition properties at these wavelengths were obtained from the NIST database [28] and are summarized below in the *Appendix*. The technique however could not be applied to the potassium doublet since the upper energy levels of the two lines are not sufficiently spaced. The two-line ratio method is highly sensitive to the intensity ratio, which includes the estimate of both the peak intensity as well as the background radiation. The sensitivity of the temperature to intensity ratio for the set of argon spectral lines used, suggests a 10% percentage uncertainty in the intensity ratio; in turn, this corresponds to uncertainty in the driver gas temperature of ±750 K.

Estimates for the driver gas temperature presented above are summarized in Table 1.

Table 1. Peak driver gas temperature estimates.

Technique	Temperature estimate (K)
Ideal isentropic compression	3743 ± 25
Blackbody approximation	3200 ± 100
Two-line method – Argon	3500 ± 750

Although there are discrepancies between the three temperature estimates, on average they indicate that the driver gas temperature is much closer to the theoretical prediction, 3800 K, than the effective temperature, 2400 K; suggesting that temperature losses are not a significant contributor to losses in the driver. Since both driver pressure and temperature have been measured for the Mach 10 flow condition, lower than expected shock speeds cannot be attributed to lower than expected driver pressure or temperature. This suggests that performance losses are more likely to be a result of pressure losses during expansion of the driver gas through the rupturing diaphragm and driver-to-driven tube area change. Future work will examine modelling of these flow processes using 2D-axisymmetric or 3D CFD analysis, to determine the primary source of this performance gap.

V. Conclusion

This study examined the initial and peak driver gas temperatures for a Mach 10 scramjet operating condition in UQ's X3 facility. The implications of this study are two-fold: firstly, initial driver gas temperature (after fill and prior to the piston stroke) in free-piston drive impulse facilities can be accurately known by monitoring the external driver tube wall temperature using surface thermocouples. Secondly, during the piston stroke, losses in the driver gas temperature are not extensive for X3; suggesting lower-than-expected performance downstream in these

facilities may be due to pressure losses from flow expansion across the driver area change. Also, the methodology established in the study to observe driver gas spectra was successfully demonstrated, providing scope for its adaptation. The established spectral composition of the driver gas will aid optimize future spectroscopic temperature studies in X3. Further experiments are required to validate the estimations of the driver gas temperature, its shot-to-shot variation, as well as, to provide an accurate description of the optical phenomena which occur in the driver section. Recommendations for this work include imaging the observing shot-to-shot variation of argon lines, validating the species of the prominent spectral lines near 587 and 672 nm, as well as, applying more sophisticated methods of estimating the spectral line intensity such as by fitting Lorentzian or Gaussian distributions to the broadened profiles.

Appendix

Table 2. Neutral argon (Ar I) transition properties and observed spectral intensity.

	Transition	Wavelength (nm)	Energy levels (eV)	Transition probability (s^{-1})	Observed spectral intensity[1] (normalized)
1	$3s^2 3p^5 4s \rightarrow 3s^2 3p^5 4p$	763.5106	11.548 → 13.172	1.22×10^8	2.7909×10^{-8}
2	$3s^2 3p^5 4s \rightarrow 3s^2 3p^5 4p$	772.4207	11.723 → 13.328	3.51×10^7	1.3314×10^{-8}
Intensity ratio (Intensity at 763 nm/ Intensity at 772 nm)					**2.0961**

[1] calculated graphically from Fig. 6b by taking the peak value of spectral intensity at the particular wavelength band and subtracting the local background

Acknowledgments

UQ's EAIT Faculty Workshop, especially Frans de Beurs and Gary Manning, for fabricating the spectroscopy fitment.

References

[1]Gildfind, D. E., Morgan, R. G., and Jacobs, P. A. *Expansion Tubes in Australia* St Lucia: The University of Queensland 2015 (to be published).

[2]Centre for Hypersonics. "X3 Expansion Tube." The University of Queensland, St Lucia, Australia, 2015.

[3]Paull, A., and Stalker, R. J. "Test flow disturbances in an expansion tube," *Journal of Fluid Mechanics* Vol. 245, No. 1, 1992, pp. 493-521.

[4]Gildfind, D. E., Sancho Ponce, J., and Morgan, R. G. "High Mach Number Scramjet Test Flows in the X3 Expansion Tube," *29th International Symposium on Shock Waves* Springer, Madison, WI, United States, 2015.

[5]Gildfind, D. E., James, C. M., and Morgan, R. G. "Free-piston driver performance characterisation using experimental shock speeds through helium," *Shock Waves*, 2015, pp. 1-8.

[6]Trimpi, R. L. *A preliminary theoretical study of the expansion tube, a new device for producing high-enthalpy short-duration hypersonic gas flows*. Washington, D. C. : National Aeronautics and Space Administration, 1962.

[7]Gildfind, D., James, C., and Morgan, R. "Performance Considerations for Expansion Tube Operation with a Shock-Heated Secondary Driver," *19AFMC: 19th Australasian Fluid Mechanics Conference*. Australasian Fluid Mechanics Society, 2014, pp. 1-4.

[8]Hans, H., and Belanger, J. "Role and techniques of ground testing for simulation of flows up to orbital speed," *16th Aerodynamic Ground Testing Conference*. American Institute of Aeronautics and Astronautics, 1990.

[9]Stalker, R. J. "A Study of the Free-piston Shock Tunnel," *AIAA Journal* Vol. 5, No. 12, 1967, pp. 1260-1265.

[10]Gildfind, D. E. "Development of high total pressure scramjet flow conditions using the X2 expansion tube," *School of Mechanical and Mining Engineering*. Vol. PhD, The University of Queensland, St Lucia, Australia, 2012.

[11]Mee, D. J. "Uncertainty analysis of conditions in the test section of the T4 shock tunnel." Technical report, The University of Queensland, St Lucia, Australia, 1993.

[12]Miller, C. G., and Jones, J. J. "Argon, carbon dioxide, and helium in a shock tube with unheated helium driver.." Langley Research Center, National Aeronautics and Space Administration, Washington, D.C. , 1975.

[13]Eichmann, T. N. "Radiation measurements in a simulated Mars atmosphere," *School of Mechanical and Mining Engineering*. PhD, The University of Queensland, St Lucia, Australia, 2012.

[14]Zander, F. "Hot wall testing in hypersonic impulse facilities," *School of Mechanical and Mining Engineering*. PhD, The University of Queensland, St Lucia, Australia, 2013.

[15]Hadas, P., Umar, A. S., Richard, G. M., Troy, E., and Tim, J. M. "Vacuum Ultraviolet and Ultraviolet Emission Spectroscopy Measurements for Titan and Mars Atmospheric Entry Conditions," *44th AIAA Thermophysics Conference*. American Institute of Aeronautics and Astronautics, 2013.
[16]Brandis, A., Morgan, R., Laux, C., Magin, T., McIntyre, T., and Jacobs, P. "Nonequilibrium radiation measurements and modelling relevant to Titan entry," *Proceedings of the 16th Australasian Fluid Mechanics Conference, 16AFMC*. Vol. 1, School of Engineering, The University of Queensland, 2007, pp. 594-601.
[17]Jacobs, C., and Morgan, R. "Radiation measurements in rarefied titan atmospheres," *47th AIAA Aerospace Sciences Meeting, Orlando, FL*. 2009.
[18]McIntyre, T. J., Bishop, A. I., Thomas, A. M., Wegener, M. J., and Rubinsztein-Dunlop, H. "Emission and Holographic Interferometry Measurements in a Superorbital Expansion Tube," *AIAA Journal* Vol. 36, No. 6, 1998, pp. 1049-1054.
[19]Devia, D. M., Rodriguez-Restrepo, L. V., and Restrepo-Parra, E. "Methods employed in optical emission spectroscopy analysis: a review.," *Ingeniería y Ciencia - Universidad EAFIT* Vol. 11, No. 21, 2014, pp. 239-267.
[20]McIntyre, T. "Pulsed Laser Imaging of Flows, Flames and Plumes." School of Physical Sciences, The University of Queensland, Brisbane, Australia, 2015.
[21]O'Byrne, S., Altenhofer, P., and Hohmann, A. "Time-resolved temperature measurements in a shock tube facility," *16th Australasian Fluid Mechanics Conference (AFMC)*. School of Engineering, The University of Queensland, 2007, pp. 1171-1176.
[22]Buttsworth, D. R., and Jacobs, P. A. "Total temperature measurements in a shock tunnel facility," *13th Australasian Fluid Mechanics Conference*. Monash University, Melbourne, Australia, 1998.
[23]East, R., and Perry, J. "A short time response stagnation temperature probe." National Advisory Committee for Aeronautics, 1966.
[24]Widodo, A., and Buttsworth, D. "Stagnation temperature measurements in the USQ hypersonic wind tunnel," *Proceedings of the 17th Australiasian Fluid Mechanics Conference (AFMC 2010)*. Vol. 248, University of Auckland, 2010, pp. 840-844.
[25]Thorne, A., Litzen, U., and Johansson, S. *Spectrophysics: Principles and Applications*. Germany: Springer-Verlag Berlin Heidelberg, 1999.
[26]Dunham, G., Bailey, J., Rochau, G., Lake, P., and Nielsen-Weber, L. "Quantitative extraction of spectral line intensities and widths from x-ray spectra recorded with gated microchannel plate detectors," *Review of scientific instruments* Vol. 78, No. 6, 2007, p. 063106.
[27]Ma, S., Gao, H., and Wu, L. "Modified Fowler–Milne method for the spectroscopic determination of thermal plasma temperature without the measurement of continuum radiation," *Review of Scientific Instruments* Vol. 82, No. 1, 2011.
[28]The National Institute of Standards and Technology (NIST). "NIST Atomic Spectra Database Lines Data." U.S. Department of Commerce., Gaithersburg, MD, 2015.
[29]Fujii, T., and Fukuchi, T. *Laser Remote Sensing*: CRC Press, 2005.
[30]Anderson, J. D. *Fundamentals of Aerodynamics (In SI Units)*. Delhi, India: McGraw Hill Education (India) Private Limited, 2014.